LABORATOIRE DE PHYSIQUE CORPUSCULAIRE

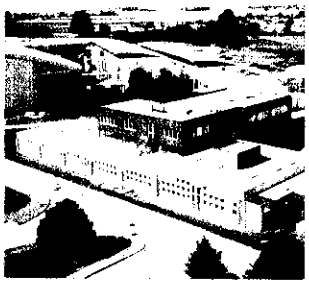

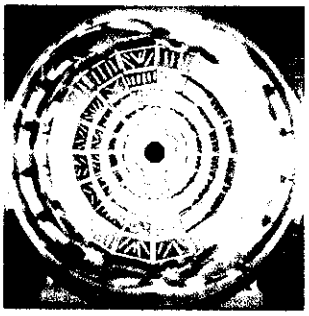

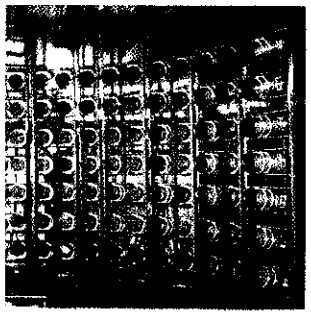

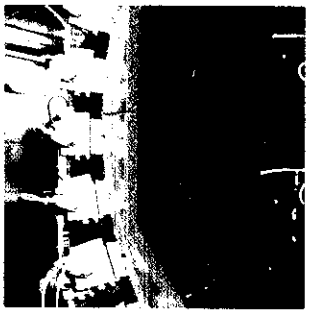

Dynamical Effects and Time Scale in Fission Processes in Nuclear Collisions in the Fermi Energy Range

J. Colin, F. Bocage, M. Louvel, G. Auger, Ch.O. Bacri, N. Bellaize, B. Borderie, R. Bougault, R. Brou, P. Buchet, J.L. Charvet, A. Chbihi, D. Cussol, R. Dayras, A. Demeyer, D. Doré, D. Durand, J.D. Frankland, E. Galichet, E. Genouin-Duhamel, E. Gerlic, D. Guinet, P. Lautesse, J.L. Laville, J.F. Lecolley, R. Legrain, N. Le Neindre, O. Lopez, A.M. Maskay, L. Nalpas, A.D. Nguyen, M. Pârlog, J. Péter, E. Plagnol, M.F. Rivet, E. Rosato, F. Saint-Laurent, S. Salou, J.C. Steckmeyer, M. Stern, G. Tabacaru, B. Tamain, O. Tirel, L. Tassan-Got, E. Vient, C. Volant, J.P. Wieleczko

INDRA Collaboration

C. Le Brun, A. Genoux-Lubain, G. Rudolf, L. Stuttgé

NAUTILUS Collaboration

October 1999

LPCC 99-20

Invited talk at the International Workshop on Nuclear Reaction and Beyond, Lanzhou, China, August 24-27, 1999

CENTRE NATIONAL DE LA RECHERCHE SCIENTIFIQUE

INSTITUT NATIONAL DE PHYSIQUE NUCLÉAIRE ET DE PHYSIQUE DES PARTICULES

INSTITUT DES SCIENCES DE LA MATIÈRE ET DU RAYONNEMENT

UNIVERSITÉ DE CAEN

- U.M.R.6534 -

ISMRA - 6, Boulevard Maréchal Juin - 14050 CAEN CEDEX - FRANCE

Téléphone : 02 31 45 25 00 - Télécopie : 02 31 45 25 49

Internet : http://caeinfo.in2p3.fr

IPNO-DR 99-58
DAPNIA/SPhN-99-58

Dynamical effects and time scale in fission processes in nuclear collisions in the fermi energy range

J. Colin[1], F. Bocage[1], M. Louvel[1], G. Auger[2], Ch.O. Bacri[3], N. Bellaize[1] B. Borderie[3], R. Bougault[1], R. Brou[1], P. Buchet[4], J.L. Charvet[4], A. Chbihi[2], D. Cussol[1], R. Dayras[4], A. Demeyer[5], D. Doré[4], D. Durand[1], J.D. Frankland[3], E. Galichet[5], E. Genouin-Duhamel[1], E. Gerlic[5], D. Guinet[5], P. Lautesse[5], J.L. Laville[2], J.F. Lecolley[1], R. Legrain[4], N. Le Neindre[1], O. Lopez[1], A.M. Maskay[5], L. Nalpas[4], A.D. Nguyen[1], M. Pârlog[6], J. Péter[1], E. Plagnol[3], M.F. Rivet[3] E. Rosato[7], F. Saint-Laurent[2,a], S. Salou[2], J.C. Steckmeyer[1], M. Stern[5], G. Tăbăcaru[6], B. Tamain[1], O. Tirel[2], L. Tassan-Got[3], E. Vient[1], C. Volant[4] J.P. Wieleczko[2],

(INDRA collaboration)

C. Le Brun[1], A. Genoux-Lubain[1,b], G. Rudolf [8], L. Stuttgé[8]

(NAUTILUS collaboration)

[1] LPC, IN2P3-CNRS, ISMRA et Université, F-14050 Caen Cedex, France.
[2] GANIL, CEA et IN2P3-CNRS, B.P. 5027, F-14076 Caen Cedex, France.
[3] Institut de Physique Nucléaire, IN2P3-CNRS, F-91406 Orsay Cedex, France.
[4] DAPNIA/SPhN, CEA/Saclay, F-91191 Gif sur Yvette Cedex, France.
[5] Institut de Physique Nucléaire, IN2P3-CNRS et Université, F-69622 Villeurbanne Cedex, France.
[6] National Institute for Physics and Nuclear Engineering, RO-76900 Bucharest-Măgurele, Romania.
[7] Dipartimento di Scienze Fisiche e Sezione INFN, Universiti Napoli "Federico II", I80126 Napoli, Italy.
[8] IRES(IN2P3-CNRS/Université Louis Pasteur) , 67037 Strasbourg Cedex, France.
a) present address: DRFC/STEP, CEA/Cadarache, F-13018 Saint-Paul-lez-Durance Cedex, France
b) present address: LPC Clermont-Ferrand, Université Blaise Pascal , 63177 Aubiere Cedex, France.

Abstract

Recent experimental results concerning heavy systems(Pb+Au, Pb+Ag, Pb+Al, Gd+U, Gd+C, Ta+Au, U+U, U+C, Xe+Sn...)obtained at Ganil by the Indra and Nautilus collaborations will be presented. A study of reaction mechanisms has shown the dominant binary and highly dissipative character of the process. The two heavy and excited fragments produced after the first stage of the interaction can experience various decay modes: evaporation, fission, multifragmentation. Howewer,

deviations from this simple picture have been found by analysing angular and velocity distributions of light charge particles, IMF's(Intermediate Mass Fragment) and fragments. Indeed, there is an amount of matter in excess emitted in-between the two primary sources suggesting either the existence of a mid-rapidity source similar to the one observed in the relativistic regime(participants) or a strong deformation induced by the dynamics of the collision(neck instability). This last scenario is explored by analysing in details the angular distributions of the fission fragments. More precisely, we observed two components: The first one is isotropic and consistent with the predictions of a statistical model, the second is aligned along the velocity direction of the fissionning nuclei and has to be compared with the predictions of dynamical calculations. In this talk, we present the probability associated to each component as a fonction of the system size, the charge asymmetry of the fission fragments, the incident energy and the impact parameter. From the statistical component we extract the temperature, the charge and the angular momentum of the fissionning nuclei. From the second component we propose a scenario to explain such process and we discuss the physical parameters which can be extracted.

1 Introduction :

Understanding the properties of nuclear matter is the most important challenge in nuclear physics. To achieve this goal, nuclei first have to be prepared in extreme conditions of excitation energy, temperature, pressure, spin and isospin. The tool used to obtain such extreme conditions is heavy ions induced reactions. For heavy systems in the Fermi energy range, two main primary fragments are formed after the collision : the primary projectile-like and the target-like fragments which can experience, depending on their excitation energies, various exit channels : evaporation of light particles, IMF emission, fission or multifragmentation.

To obtain physical information about the projectile-target nuclear interaction and the two excited primary fragments, the characteristics of all detected fragments and particles can be compared with those predicted by various models. For example, statistical models are often used [1], [2], [3], [4], [5] to describe the decay of the primary fragments. The comparison of experimental data with such models first implies to test whether all degrees of freedom (thermal, chemical and shape equilibrium) are equilibrated and whether there is no coupling left between entrance and exit channels . In this work, we present some results concerning one fixed exit channel : the breakup of the projectile-like source in two fragments for which we will give strong evidence for the occurrence of two types of mechanisms, namely standard fission and aligned breakups.

First of all, we present an illustration about the binary aspect of the process and next the different angular distributions which put forward privileged directions corresponding

to aligned breakups. In order to disentangle standard fission and non-statistical breakup a method is lastly proposed, which allows to quantify the relative importance of these mechanisms as a function of the target and projectile sizes, the incident energy, the violence of the collision and the asymmetry of the breakup.

2 Reaction mechanisms :

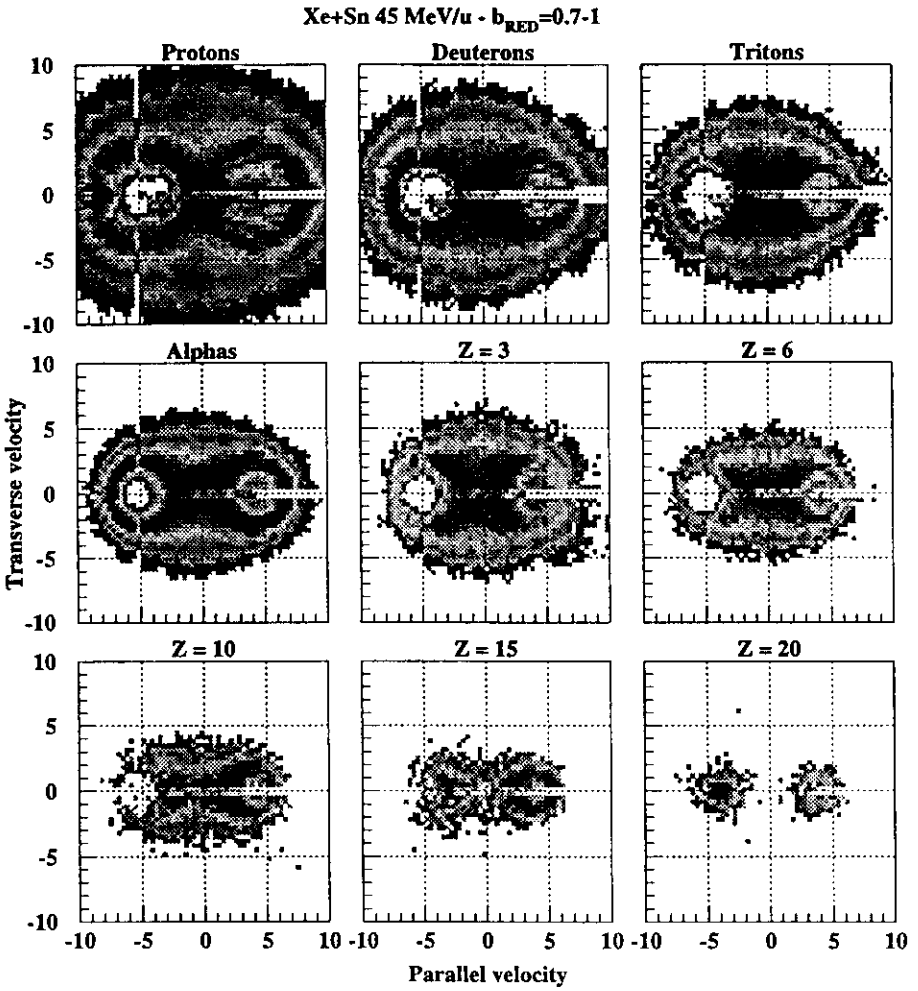

Figure 1: Vpar-Vper (cm/ns) velocity plots, in the center of mass, for the Xe+Sn system at 45 MeV/u for peripheral collisions. The different panels present various types of reaction products : light charged particles (p,d,t,α) and fragments.

For heavy systems at incident energies close to 30 MeV/u, most of the collisions correspond to binary processes [6], [7]. This aspect is illustrated on fig.1 where the transverse

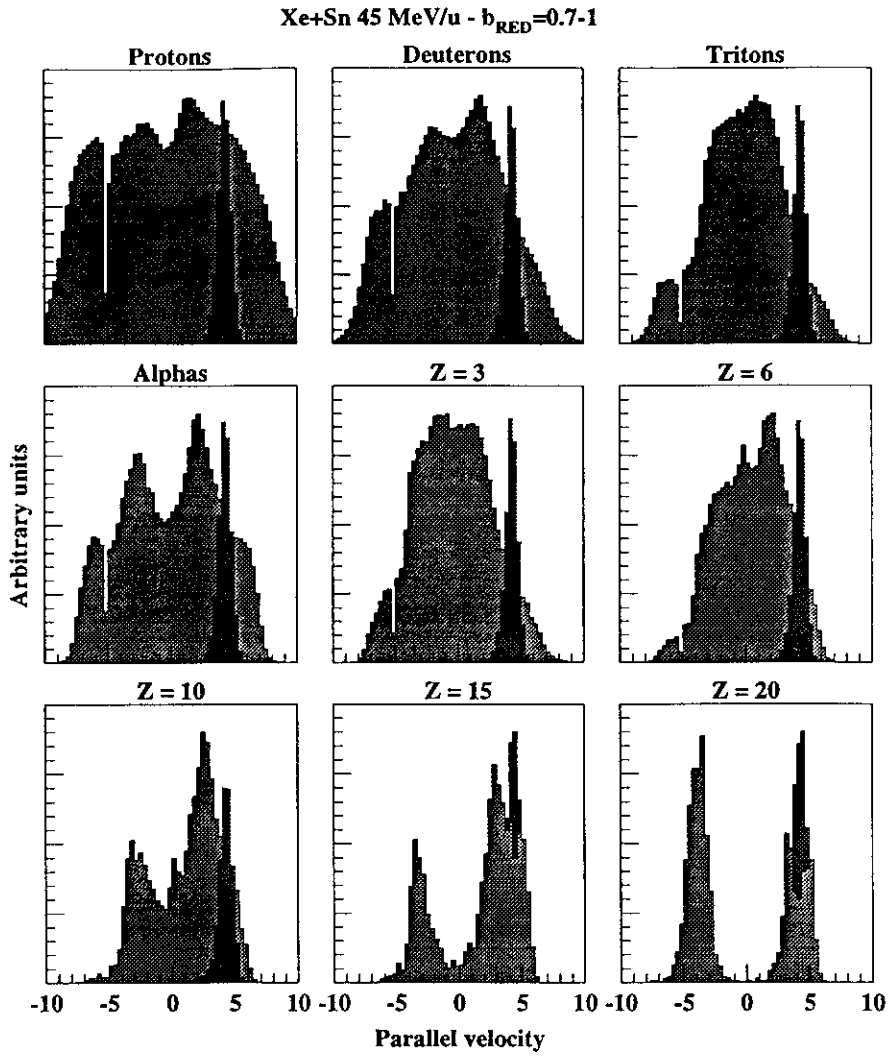

Figure 2: Xe+Sn system at 45 MeV/u, peripheral collisions: parallel velocity distribution (cm/ns) for the same type of reaction products as in fig.1 (light grey area) and for the heaviest fragment detected in coincidence (dark grey area).

versus parallel velocity invariant plots ($V_{par} - V_{per}$ correlations) for peripheral collisions are shown for protons, deuterons, tritons, alpha particles, and fragments with charge 3, 6, 10, 15, 20. The impact parameter b, or the reduced one b_{red}, has been estimated with a method based on the transverse energy of light charged particles $E_t^{12} = \sum E_i \sin^2(\theta_i)$ (where E_i is the kinetic energy of the particle i and θ_i its angle relative to the beam direction) [8], [9], [10], [11] and[12].
First it appears clearly that most of the collisions correspond to binary processes. We observe two nice circles around the projectile and target parallel velocities ($|V_{par}| = 4.5\ cm/ns$), except for the reaction products emitted by the target which are too slow to be detected or identified. Also we can see an amount of matter in excess between the two primary fragments. To go into detail, we have plotted on fig.2 the parallel velocity distributions of the particles and fragments (light grey area) coïncidentally detected with a projectile-like residue (dark grey area). We observe that the forward parts ($V_{//} > 0$) of the velocity distributions (not influenced by threshold effects) are not symmetrical with

respect to the projectile-like residue velocity: These fragments are often slower than the PLF which is also the heaviest fragment. Moreover, a large number of fragments and light charged particles are emitted between the two primary fragments. Such a hierarchy suggested to us to study the fragment production against their size by means of angular correlations. The mid-rapidity particles and fragments have already been studied in different works [13], [14], [15],[16], [17], [7], [18], [19].

3 Evidence for aligned breakups :

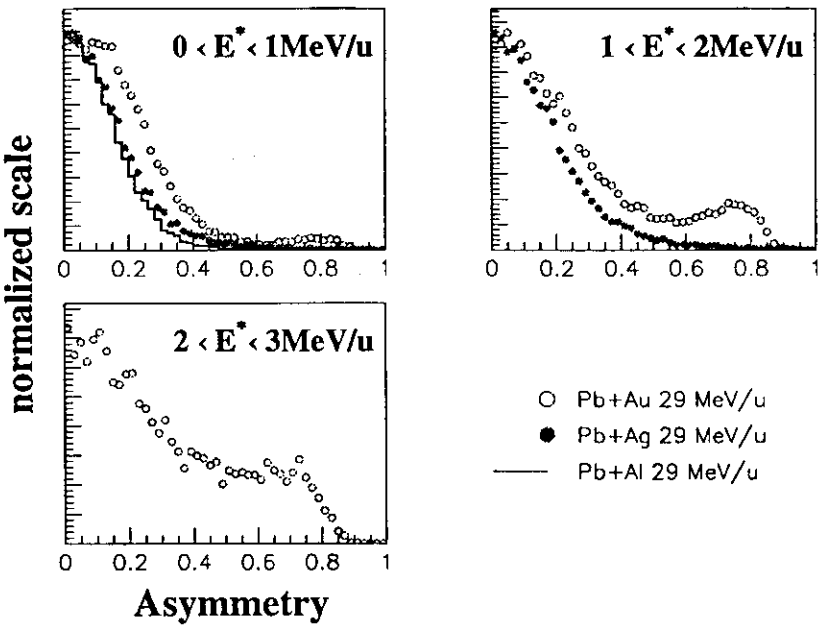

Figure 3: Asymmetry distributions for fission fragments of a Lead projectile-like after a collision with a Gold target (open circles), a Silver target (full circles), or a Aluminium target (line). These distributions are arbitrarily normalised at asymmetry=0.

We will now focus our study on the binary breakup of the PLF for various systems and incident energies. In this purpose we select the events with two fragments emitted forward in the center of mass and assume that these two fragments result from the fission of the PLF; we thus reconstruct the fissioning nucleus, its velocity and the fission axis (the axis between the two detected fragments). In order to take into account the influence of the size of the two fission fragments, observed in fig.1 and 2, this axis is orientated from the light to the heavy fragment (fig.5). The reaction plane is defined by the recoil direction

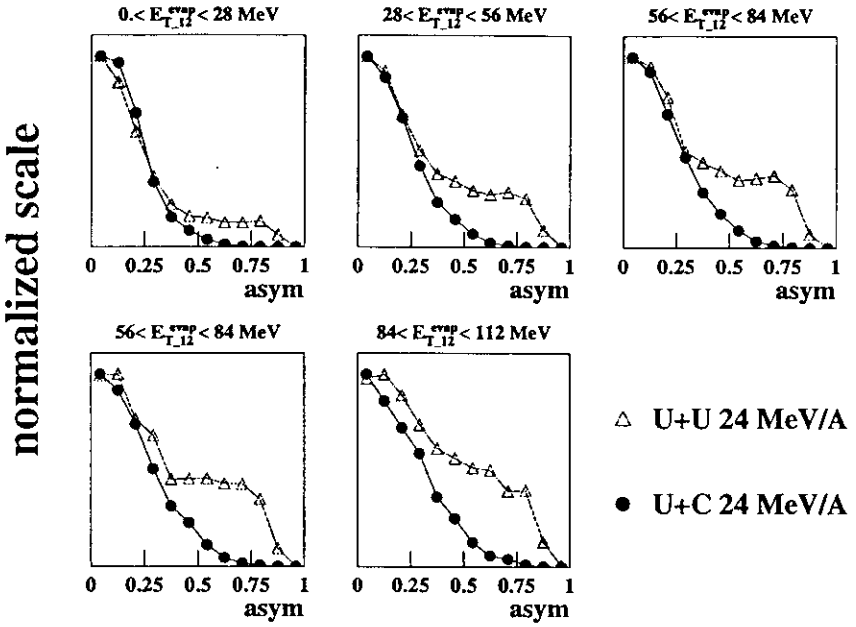

Figure 4: Asymmetry distributions for fission fragments of a Uranium projectile-like after a collision with a Uranium target (open triangles) or a Carbon target (full circles). These distributions are arbitrarily normalised at asym=0.

of the PLF and the beam axis. We first present some direct observables: the asymmetry distribution of the fission fragments $\eta = (Z_1 - Z_2)/(Z_1 + Z_2)$ for different projectile target combinations in fig.3 and fig.4. For light target(carbon or aluminium) the fission is mainly symmetrical (asymmetry=0) but for heavy target an important contribution for highest asymmetries (asymmetry=0.75) is observed. This component increases with the charge of the target and the violence of the collision. To study the space distributions of the fission fragments, different angles are used. The "proximity angle" θ_{prox} (fig.5) is the angle between the direction of the PLF velocity and the fission axis. In the case of a "standard" fission, all directions are allowed and a flat $dN/d\cos\theta_{prox}$ distribution is expected. Spin effect, if any, favours the reaction plane, thus the recoil axis, and then increases slightly and symmetrically the distribution for $\cos(\theta_{prox}) = \pm 1$. In fig.6 we present the experimental $\cos(\theta_{prox})$ distributions associated with the PLF binary breakup for Pb projectile, different targets (Al, Ag and Au) and different breakup asymmetries η. We observe that for the lightest target (Al), the distributions obtained are symmetrical with respect to zero, so they correspond to what is expected in "standard" fission of a rotating nucleus. The holes seen for $\cos(\theta_{prox})$ equal -1 are due to detector effects, and are non physical : this angle would correspond to a binary breakup aligned with the PLF recoil axis and thus to a detection of the two fragments in the same detector. Such configurations can not be detected, nor corrected from detector effects. For the silver target, in symmetrical fission the distribution is also compatible with a "standard" fission but for

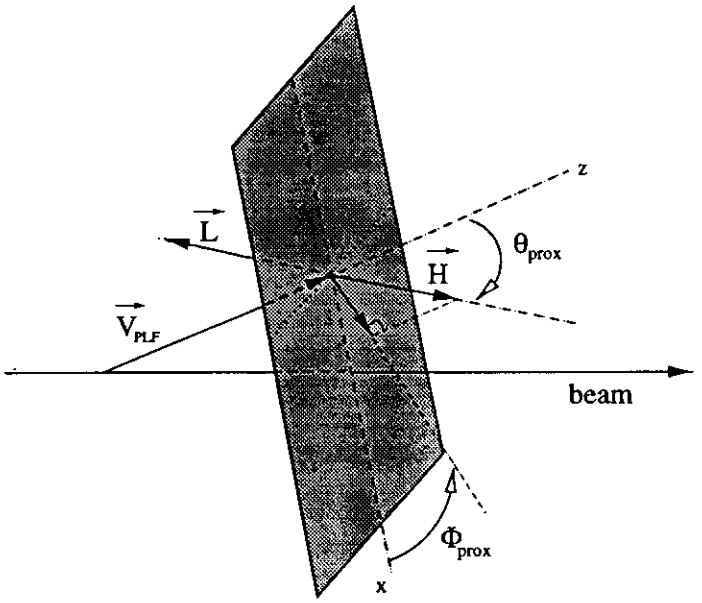

Figure 5: θ_{prox} : angle between the breakup axis, orientated from the light L to the heavy fragment H, and the recoil velocity of the projectile like fragment (noted V_{PLF}) reconstructed with the two fission fragments.

asymmetrical fission with η >0.2 , we observe that the distributions are not symmetrical : $\cos(\theta_{prox}) = +1$ is favoured, which corresponds to a breakup aligned on the PLF recoil axis, with the heavy fragment faster than the light one. For the Au target the same effect is clearly seen even for the smallest breakup asymmetry.

To check the influence of the experimental set-up and of the projectile size, we present in fig.7 the same observable obtained with the INDRA multidetector for the binary breakup of Gd impinging on two different targets : a light target (C) and a heavy one (U). The observations are exactly the same and then depend neither on the detector (NAUTILUS or INDRA) nor on the studied projectile (Pb or Gd). For light targets (C, Al), we mainly observe "standard" fissions of the incomplete fusion nuclei. For heavier targets (Ag, Au, U), we observe the "standard" fissions of the PLF only for symmetrical breakups.

Thus, for heavier targets and greater asymmetry, the breakup axis is preferentially aligned with the separation direction of the two primary fragments (TLF and PLF), the lighter fragment emitted by the PLF being located between the heavy one and the TLF. This effect increases with the size of the target and the asymmetry of the PLF breakup. This privileged direction, depending upon the charges of the PLF fragments, thus suggests a target effect. Aligned binary breakup of the PLF has been previously observed at Fermi energies [20], [13] and also at lower energies [21], [22], [23]. Such a behaviour can not be understood in a classical approach of "standard" fission because this statistical description presupposes that there is no coupling left between entrance and exit channels.

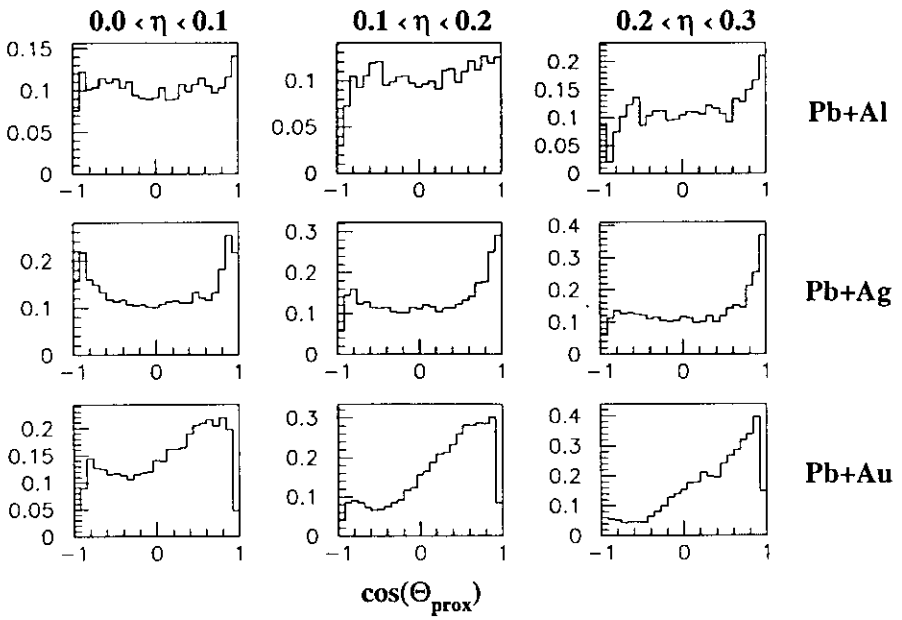

Figure 6: Pb + "X" at 29 MeV/u for peripheral collisions ($E^* \leq 1\ MeV/u$) (NAUTILUS). $\cos(\theta_{prox})$ distributions associated with the fission of Pb-like fragment, for different "X" targets and for different asymmetries of the fission fragments. The rows correspond respectively to Al, Ag, Au targets, and the columns to different asymmetries of the fission fragments.

The only privileged directions compatible with this description are the reaction plane due to spin effects. The asymmetry distributions and the alignement that we observed suggest the breakup of a deformed projectile-like source.

4 Competition between fission and non-statistical binary breakup :

The distributions plotted on fig.6-7, can be viewed as the sum of two components : the first one, symmetrical with respect to 0, which could be associated to standard fission, and the second one peaked at 1, related to non-statistical breakup. This simple assumption will be discussed later. The relative weights of these two components depend on the target size, on the projectile size and the breakup asymmetry. In order to obtain the first component, we symmetrised around $\cos(\theta_{prox}) = 0$ the backward part ($cos(\theta_{prox}) < 0$) of the experimental distribution, supposing thus that this part is not influenced by non-statistical breakups : the $cos(\theta_{prox})$ distribution are indeed expected to be symmetrical

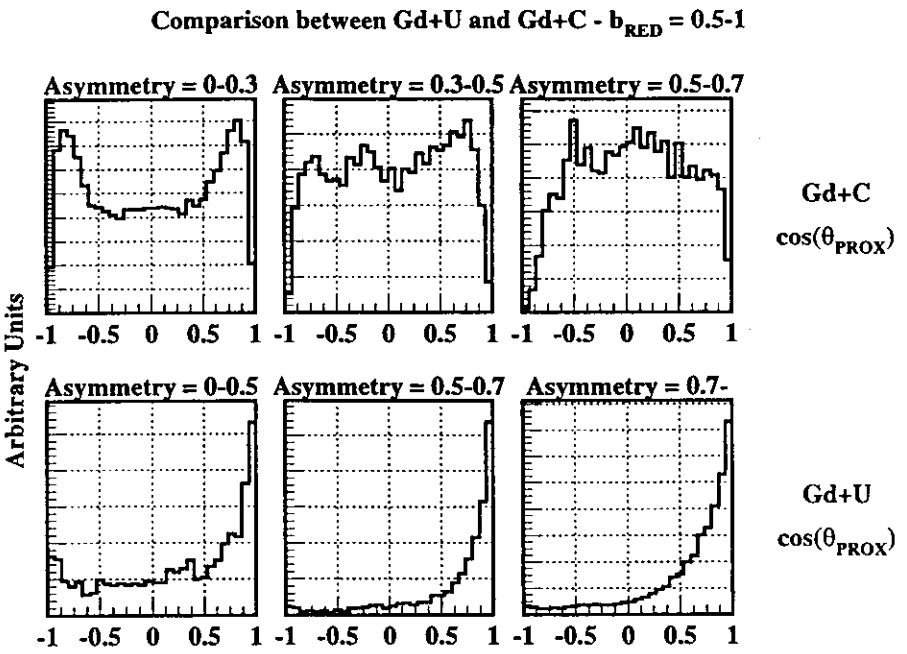

Figure 7: Gd + "X" at 36 MeV/u for peripheral collisions (INDRA). $\cos(\theta_{prox})$ distributions associated with the fission of a PLF for a Gd projectile and for different "X" targets and for different asymmetries of the fission. The columns correspond to different asymmetries of the fission-fragments, the lines respectively to C and U targets.

in the case of standard fissions. The aligned contribution is then obtained by subtracting this reconstructed "standard" fission distribution from the total experimental distribution. The result of this procedure is shown in the right column of fig.8, while the initial distribution are presented in the central one, for different breakup asymmetries of the Pb+Ag system. The relative importance of these two contributions is given by the percentage of aligned breakup. In the case of symmetric breakup, only 5% of non-statistical breakups are found (upper row fig.8). This percentage increases with the asymmetry and reach 22% for an asymmetry of 0.35 which corresponds to a charge value of 54 for the heaviest fragment and 26 for the lightest one.
In the left column, we have plotted the out-of-plane angle $\cos(\theta_{spin})$ distributions. This angle is defined as the angle between the breakup axis and the aligned spin axis (fig.9). On the one hand, the higher the value of the spin of the fissioning nucleus, the more the fission fragments are emitted in the reaction plane. On the other hand, the non-statistical breakups aligned with the PLF recoil axis also favour the reaction plane. These two effects contribute to the the "bell shape" curve obtained in the left column in fig.8, because the reaction plane corresponds to $\cos\theta_{spin} = 0$, and their relative contributions are difficult to estimate. In this particular case where the target is not very heavy, the probability of aligned breakup is relatively low. The width of the $\cos\theta_{spin}$ distributions, often used to

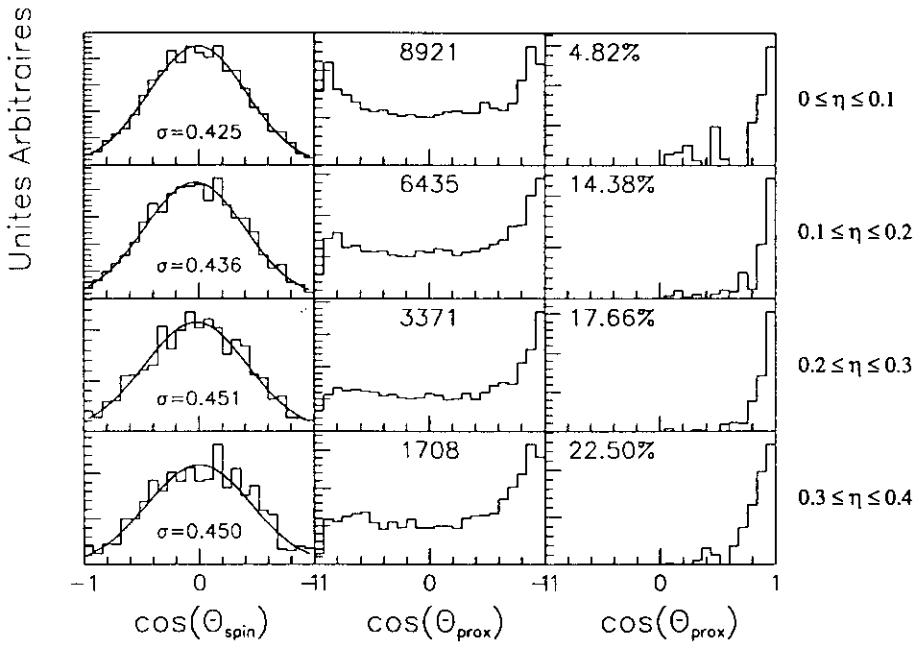

Figure 8: Pb + Ag at 29 MeV/u for peripheral collisions (NAUTILUS). Left panel: $\cos(\theta_{spin})$ distributions associated with different fission asymmetries (see text for the θ_{spin} definition). Central panel: $\cos(\theta_{prox})$ distributions associated with different fission asymmetries. The number of experimental events is indicated in each case. Right panel: $\cos(\theta_{prox})$ distributions obtained after subtraction of the reconstructed "standard" fission distribution from the total distribution. The percentage of aligned fission relative to the total events for the same asymmetry is given on each panel. (see text for details).

measure the angular momentum of the fissioning nucleus [24], will then give only slightly overestimated spin values.

For other systems and higher asymmetries, the non-statistical breakup could become dominant and the previously used method does not allow to separate the two contributions (see fig.6 for Au target), nor to measure the angular momentum of the fissioning nuclei directly with the $\cos\theta_{spin}$ distributions. It appeared more appropriate to use another angle, ϕ_{plane}, defined as the angle between the breakup axis projected into the reaction plane and the recoil velocity of the PLF (fig.9). For a "standard" fission, a ϕ_{plane} distribution is expected to be flat. Fig.10 presents such distributions for Xe+Sn at 25 MeV/u for the most peripheral events. For symmetrical breakup (left upper plot on fig.10), the ϕ_{plane} distribution is roughly flat in agreement with the expectations of a "standard" fission, but for asymmetrical breakups (right plots on fig.10), a large contribution emerges for small

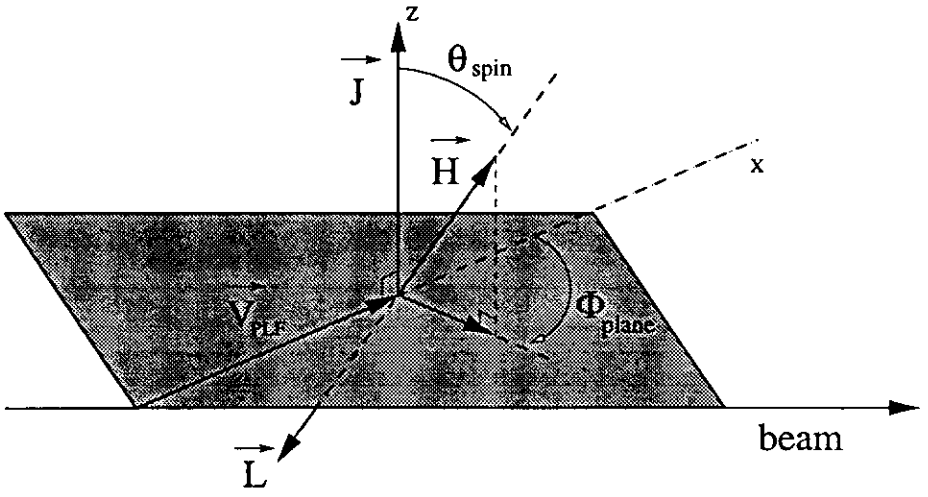

Figure 9: θ_{spin} definition : angle between the fission axis oriented towards the heaviest fission fragment H and the reaction plane deduced from the recoil velocity of the projectile like fragment (labelled V_{PLF}) and the beam velocity. ϕ_{plane} definition : angle between the fission axis projected on the reaction plane and the recoil velocity of the projectile like fragment .

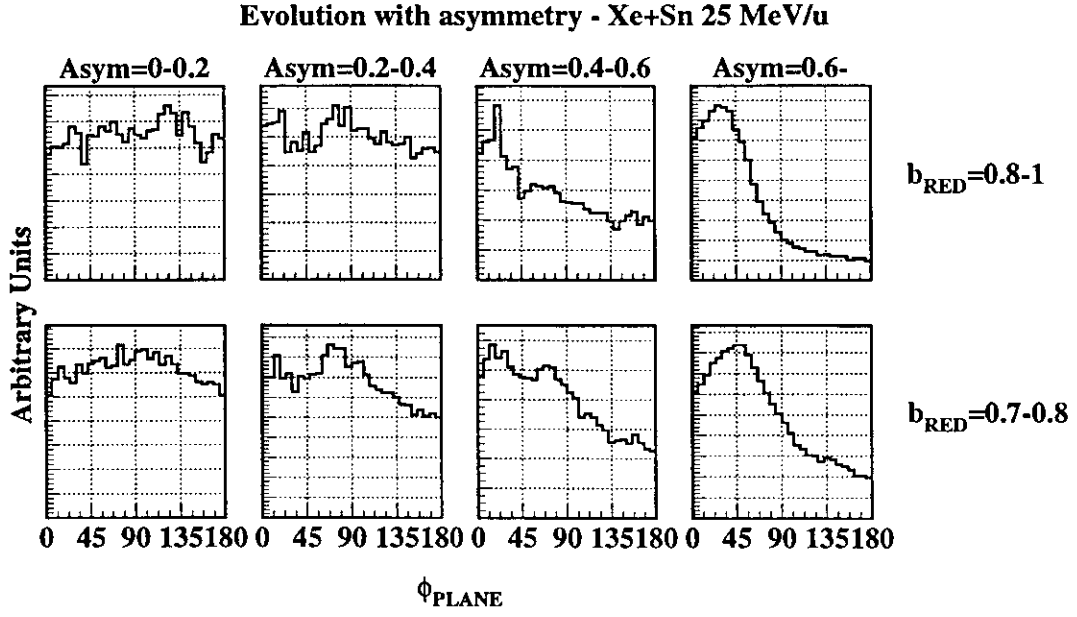

Figure 10: Xe+Sn system at 25 MeV/u. ϕ_{plane} angle distributions for different values of the fission asymmetry and for two ranges of impact parameter (b_{RED}=0.8-1.and b_{RED}=0.7-0.8).

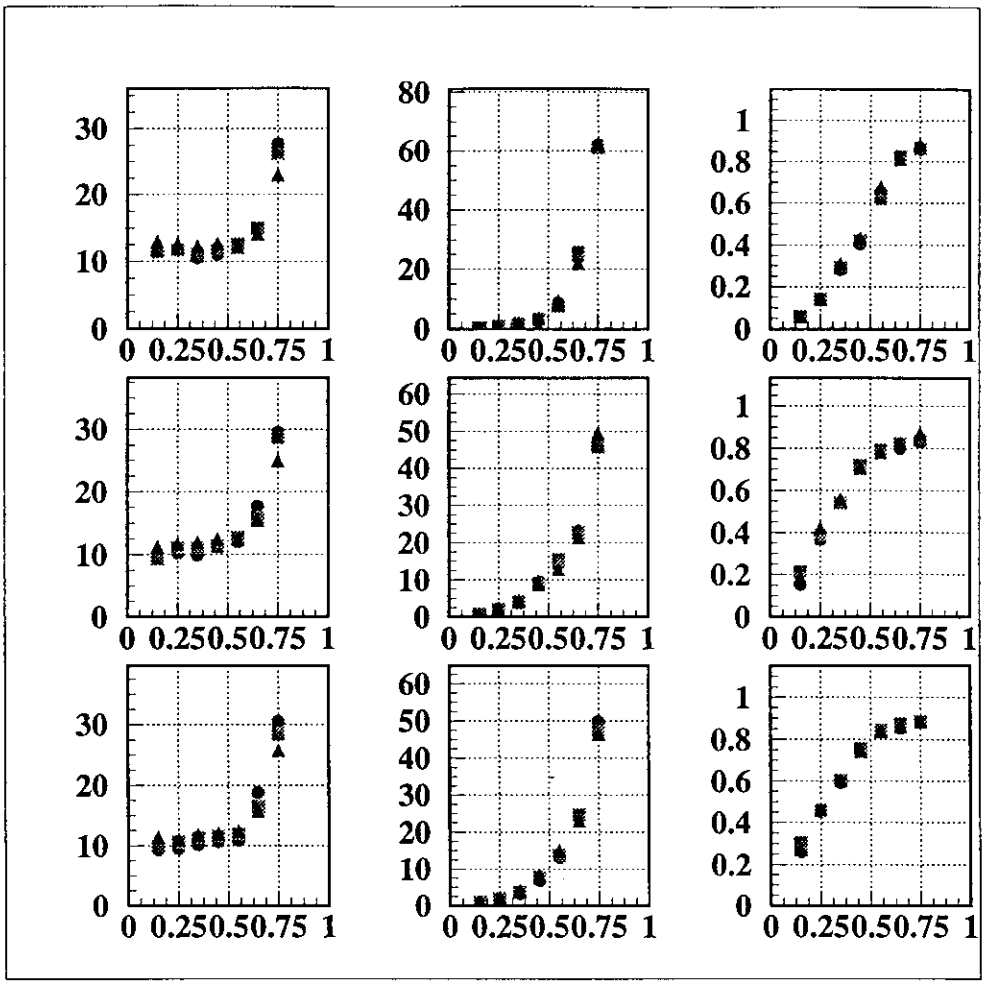

Figure 11: Probability distribution of asymmetry associated with "standard" fission (left column), to "aligned" breakup (central column) and the ratio between "aligned" and "standart" fissions for Xe+Sn system for various incident energies (circles 50 MeV/u, squares 45 MeV/u, triangles 39 MeV/u) and for various impact parameters. The different rows correspond to different impact parameter bins (upper: b_{RED}=0.8-1, middle: b_{RED}=0.7-0.8, lower: b_{RED}=0.5-0.6)

values of ϕ_{plane} associated with aligned breakups. Also we observe another contribution around ϕ_{plane} = 90 degrees. This contribution perpendicular to the PLF-TLF separation direction is due to Coulomb repulsion between the target and the fission fragments [23], [25], (see later fig.14). The two angles θ_{spin} and ϕ_{plane} belong to spherical coordinates in the PLF frame and thus are independent : we can select the events associated with the flat part of the ϕ_{plane} distribution, and look at the corresponding $cos(\theta_{spin})$ distributions. Like those lying in the backward part of the $cos(\theta_{prox})$ distributions, these events may be considered as standard fissions of PLF's. We will discuss the pertinence of this assumption later. Since the ϕ_{plane} distributions are not influenced by spin effects, these events are even characteristics of the standard fission component. The $cos(\theta_{spin})$ distributions obtained are then only influenced by spin effects and this allows to estimate the angular

momentum of the projectile like fragments which experience standard fissions. Of course, such measurement having no significance for non-statistical breakups. In order to obtain the probabilities associated with these two types of mechanisms, a method similar to that previously proposed with the $cos(\theta_{prox})$ distributions (percentage on fig.8) has been used on the ϕ_{plane} distribution : the flat part of the distribution is assimilated to the statistical component and subtracted from the total to get the aligned breakup component. The probabilities of the two phenomena are presented (fig.11) against the breakup asymmetry for the Xe+Sn system at various incident energies and for several impact parameters. We first observe that the probabilities of both types of breakup do not depend on the incident energy. Moreover, while the probabilities of statistical fission do not change with the impact parameter, those of aligned breakups exhibit a strong evolution : we observe only asymmetrical breakups in peripheral events and symmetrical breakups appears only for more central collisions. So it seems that the violence of the collision influences more the aligned breakups than the statistical fissions. For this system, the "standard" fission represents only 25% of the total number of events whatever the incident energy and impact parameter. Most events correspond to aligned breakups and can not be compared to statistical models. The physical information, like fission probabilities or angular momentum, obtained with such models would be wrong [26]. So it is very important to study not only the global observables, like multiplicity or charge distributions, but also in detail the reaction mechanisms which lead to binary breakup, by looking for example at the angular distributions and relative velocity distributions.

5 Comparisons with a statistical prescription:

The method used to quantify the two mechanisms is entirely based on the assumption that the backward part of the $cos(\theta_{prox})$ distributions, or the flat part of the ϕ_{plane} distributions, corresponds to "standard" fissions. We want now to verify that the probabilities of these events are also compatible with a statistical prescription. These probabilities have been compared to those predicted by the "transition state model" [2], [27] with the fission barrier values given in [28]. This model calculates the probability of observing a given fission asymmetry for a fixed charge of the fissioning nucleus, a fixed temperature and a fixed angular momentum.

It is applied for different systems (Gd+U, Gd+C and Xe+Sn) and compared to the experimental data (fig.12). Although the variations of the breakup probabilities with asymmetry are very different for the three studied PLFs, they are rather well reproduced by the calculation with reasonable values of charge, temperature and spin of the fissioning nuclei. The agreement with statistical model predictions for various PLFs can be considered as solid proof of the validity of our method to separate statistical fissions and aligned breakup : all variables associated with the first type of events are rather well reproduced by statistical models, while these models fail in accounting for the angular distributions obtained in the second type of breakups.

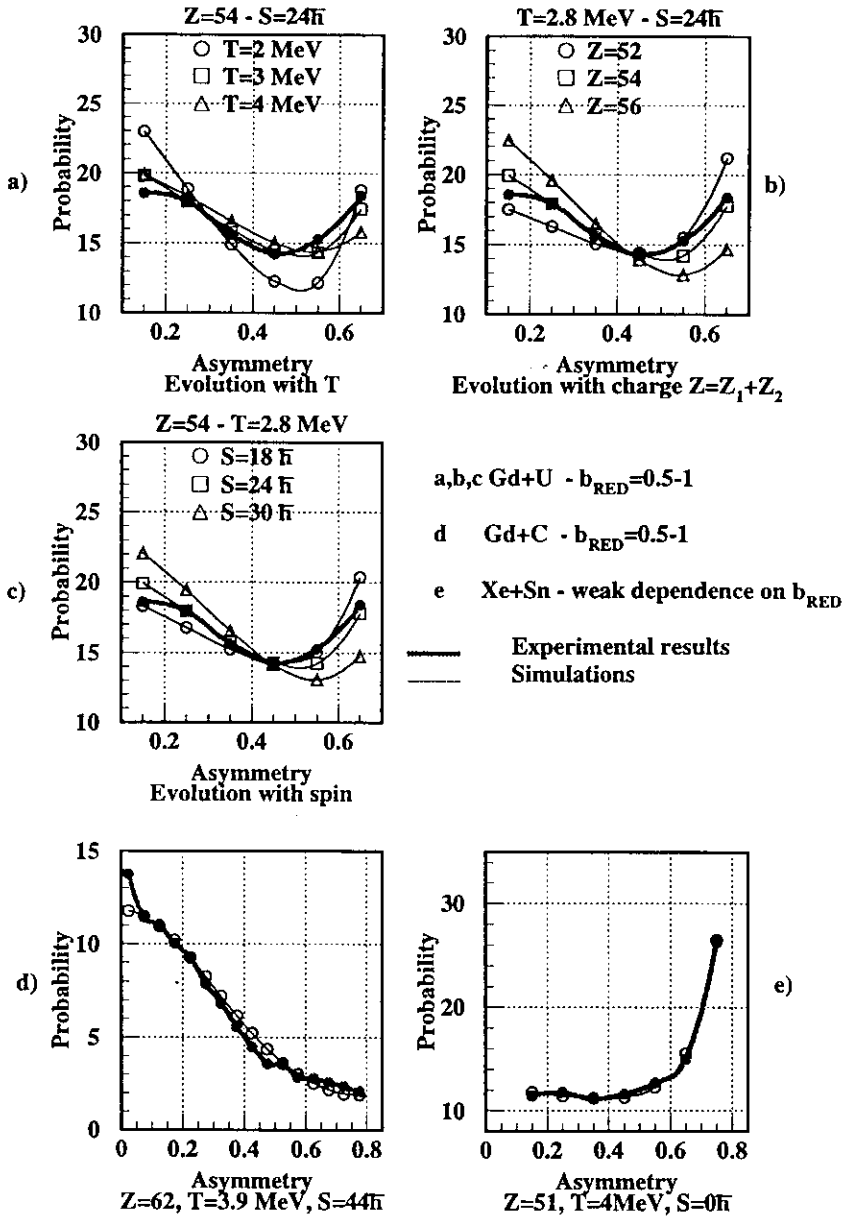

Figure 12: "Standard" fission probability against breakup asymmetry for different systems and impact parameters integrated from b_{max} (peripheral collisions) to $0.5b_{max}$ for the Gd+U system at 36 MeV/u (a,b,c). a: evolution with the temperature of the fissioning nucleus. b : charge of the fissioning nucleus. c: spin of the fissioning nucleus. d: Gd+C system at 36 MeV/u. e: Xe+Sn system at 45 MeV/u. The full symbols correspond to the data, the open symbols to the calculations.

For the Gd+U system, the shape of the curve is very sensitive to the "free" parameters (charge, temperature and spin of the fissioning nuclei). For example we can see a large

difference when the temperature is increased from 2 to 3 MeV (fig.12a). In fact, we have some more constraints on the "free" parameters. The $\cos(\theta_{spin})$ distributions, associated with the flat part of the ϕ_{plane} distributions, give us a constraint on the ratio $J/\sqrt{T}$ [24]. Moreover, the charge of the fissioning nucleus is necessarily greater than or equal to the sum of the charges of the two detected fragments. The results of our comparison show that for Gd+U system at 36 MeV/u, the experimental probability distribution is compatible with the calculated one for the fissioning nucleus at the saddle point with charge 54, temperature 3 MeV and spin $24\hbar$. The charge 54 is equal to the sum of the charges of the detected fission fragments. So it suggests that the fission takes place at the end of the decay process. [29], [30]

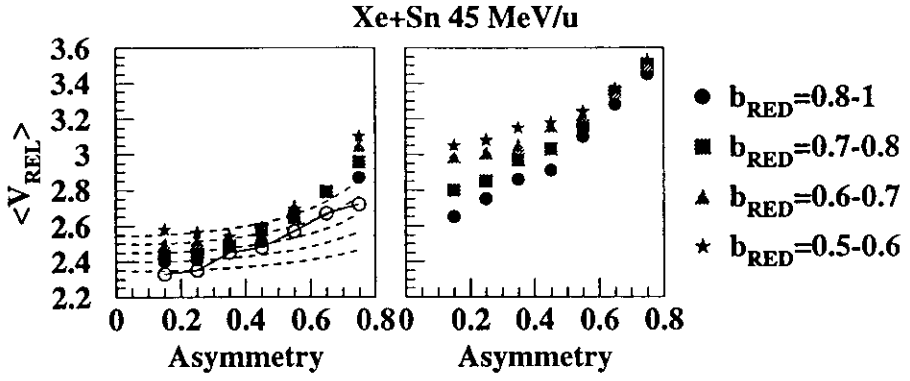

Figure 13: Relative velocities against fission asymmetry for different impact parameters for the Xe+Sn at 45MeV/u. The full symbols correspond to mean values. Left column: distribution associated with the "standard" fission, the open circles concern the most probable value of the relative velocity for b=0.8-1. The dashed lines correspond to different temperatures 2, 4, 6, 8, 10 MeV in the calculation. Right column: distribution associated with the aligned component.

Lastly, we studied the relative velocity between the two fission fragments of the PLF. We compared the values obtained for the experimental "standard" fission with the prediction of a simple Coulomb repulsion and also to the values obtained for the aligned breakup in order to extract some quantitative information on this last process (fig.13). The contribution of aligned breakup to the relative velocity distribution is obtained by subtracting the contribution associated with the "standard" fission from the total relative velocity distribution. The dashed lines on fig.13 correspond to the value of relative velocities obtained with the previous calculation using different values of the temperature of the fissioning nucleus. For the highest asymmetries ($\eta > 0.5$) and the lowest impact parameters, the experimental relative velocities for "standard" fission on fig.13a are greater than the expected one, suggesting that the fissioning nucleus has a high temperature. Howewer this possibility is in contradiction with the conclusion of a fission at the end of the decay

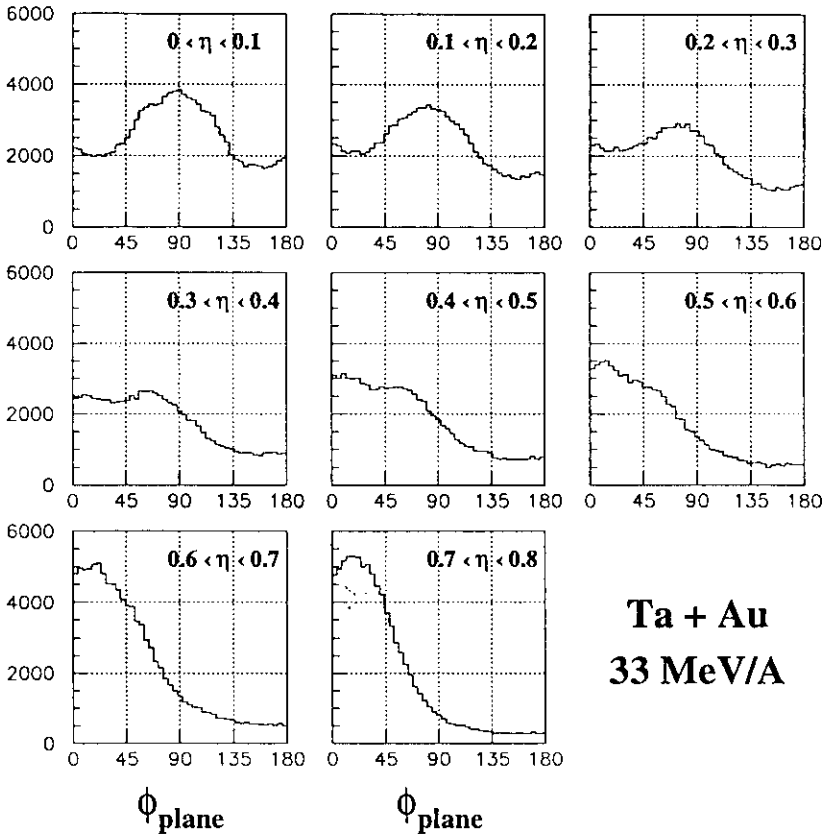

Figure 14: Ta + Au 33 MeV/u (INDRA). $\cos(\theta_{prox})$ distributions associated with the fission of Ta-like fragment, for different asymmetries of the fission fragments.

process, obtained with the analysis of the probability distributions of asymmetry. In spite of this inconsistency for few extreme asymmetries and impact parameters, the velocities remains roughly compatible with the calculation for the most part of the "standard" fission component. On the contrary, in fig.13b, the relative velocity values are always higher for the aligned component. Even for peripheral events the relative velocities are higher than those obtained by the calculation with extreme values of the temperature. They also show a strong evolution with the impact parameter, mainly for the symmetrical fissions. These values and these evolutions can not be understood within a statistical prescription. Recently, we have applied these methods on another system Ta+Au at 33MeV/u. The different fission processes appear clearly in fig.14. The flat ϕ_{plane} component, compatible with statistical fission is very important for this system, the aligned component with respect to the PLF velocity (ϕ_{plane}=0) is cleary observed for asymmetrical fissions and the aligned component with respect to the perpendicular direction of the PLF velocity in the reaction plane (ϕ_{plane}=90) is cleary observed for symmetrical fissions. We have also

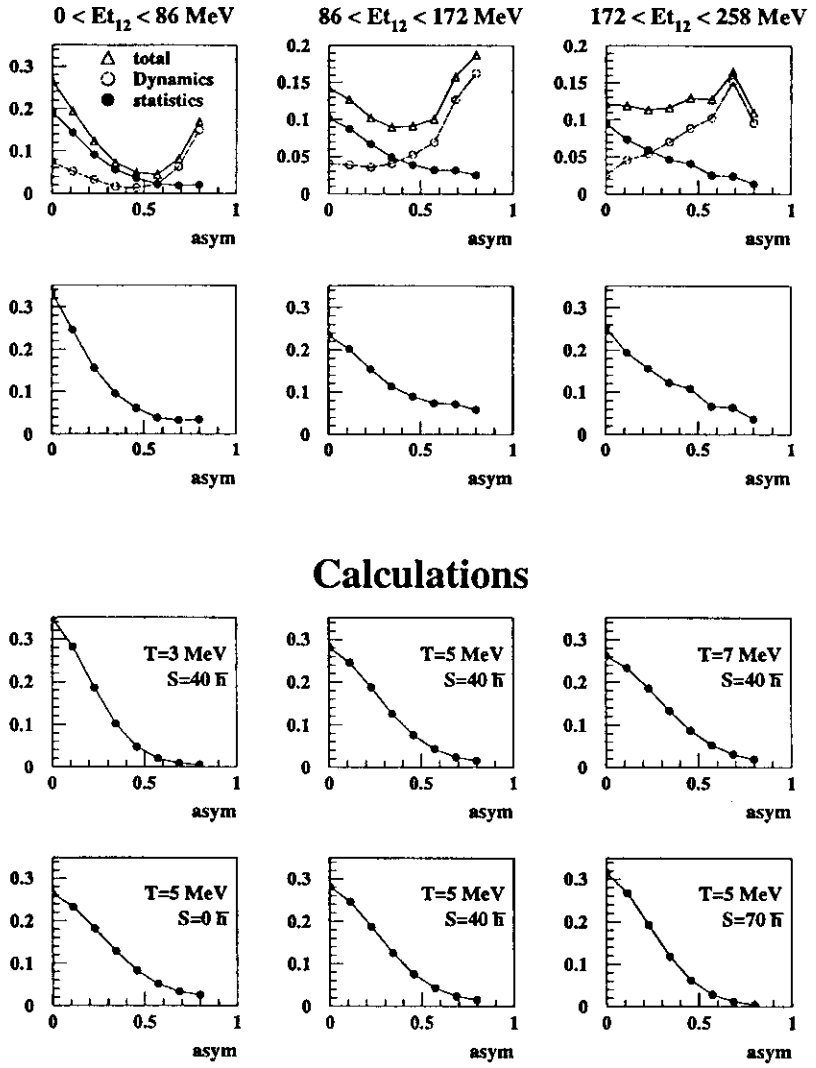

Figure 15: Asymmetry distribution associated with the fission fragments of a Tantalum projectile-like after a collision with a gold target for different values of transverse energy of light charged particles (impact parameter).

studied in fig.15 the distribution of asymmetry associated with the statistical component. The comparison with a statistical calculation is promising.
All these observations suggest that the aligned fission originates from very strong deformations of the projectile during its interaction with the target. Just after the collision the deformation is very large and is amplificated by the nuclear potential or by the coulomb

potential of the target. The projectile-like fragment goes inevitably towards fission : the PLF does not return to his equilibrated shape before its breakup, like in the case of a "standard" fission. Its deformation is as large (or even more) as the deformation of the same nucleus at the saddle point in a "standard" fission process. The process is continuous, so the relative velocity associated with the deformation at the saddle point is different from zero. This velocity can be considered as a deformation velocity which is related to the viscosity of nuclear matter. Thus, the measured relative velocity between the fission fragments is higher than in a "standard" fission. This observed relative velocity is the addition of the Coulomb repulsion and the deformation velocity of the PLF, which then puts an experimental constraint on nuclear viscosity.

6 Summary:

In heavy ion collisions, the reaction mechanisms are really complex. We have given evidence for the binary aspect of the collisions but also for different dynamical origins of particles and fragments. In this work we focused our study on the decay in two fragments of the projectile-like fragment and we compared this process with a "standard" fission scenario. By using all the information obtained with 4π arrays, (angular distributions, asymmetry of the fission fragments) two fission components could be extracted. One component is compatible with the "standard" fission. This component has been compared to calculations using statistical hypothesis and all the observables are in a quite good agreement. From this comparison we have derived the characteristics of the fissioning nucleus (charge, temperature and spin) at the saddle point. The second component is aligned on a direction relative to the entrance channel: the direction of the velocity of the PLF (nuclear potential influence of the target on the fission process) or the perpendicular direction of this PLF velocity in the reaction plane (coulomb potential influence of the target on the fission process). The relative weight of each component depends on the size of the systems and on the asymmetry of the fission fragments but not on the incident energy. The aligned fission represents, for example, 75% of the total number of fission events for the Xe+Sn system and can not be reproduced by calculations using statistical hypothesis. The measured relative velocities between the two fission fragments for this component are very high and depend on the impact parameter. The observables associated with aligned fission have to be compared with dynamical calculations in a further analysis.

Acknowledgments:

The author would like to warmly thank his friends from LPC Caen specially Frédéric Bocage, Jacques Normand, Daniel Cussol and the NAUTILUS and INDRA collaborations.

References

[1] Weisskopff et al., Physical Review C52(1937) 295

[2] N. Bohr et al., Physical Review 56(1939) 426

[3] L.G. Moretto et al., Physical Review Letters 74 N9 (1995) 1530-1533

[4] L.G. Moretto et al., Physics Reports 287 (1997) 249

[5] K. Tso et al., Physical Letters B361 (1995) 25-30

[6] J.F. Lecolley et al., Physics Letters B325 (1994) 317

[7] V. Métivier Thèse Université de Caen (1995)
V. Métivier et al., submitted at Nuclear Physics A

[8] F.Bocage Thèse Université de Caen (19998)

[9] E. Plagnol et al., Preprint IPNO DR 99-10, submitted to Phys. Rev. C

[10] J. Peter et al., Nuclear Physics A519 (1990), 611-630

[11] L. Phair et al., Nuclear Physics A548 (1992), 489-509

[12] C. Cavata et al., Physical Review C42 N4 (1990), 1760-1763

[13] C.P. Montoya et al., Physical Review Letters 73 N23(1994) 3070-3073

[14] W.G. Lynch, Nuclear Physics A583(1995), 471-480

[15] T. Lefort et al. (INDRA collaboration), Preprint LPCC 98-15, Submitted to Nuclear Physics A.

[16] D.Doré et al. (INDRA collaboration), Proceedings of the XXXVIth Winter Meeting on Nuclear Physics, Edited by I.Iori, 26-31 January 1998, Bormio, Italy, 381-394.

[17] E. Galichet et al. (INDRA collaboration), Proceedings of the XXXVIth Winter Meeting on Nuclear Physics, Edited by I.Iori, 26-31 January 1998, Bormio, Italy, 410-424.

[18] J. Lukasik et al., Physical Review C vol. 55, Num. 4 (1997)

[19] O. Tirel Thèse Université de Caen (1998)

[20] J.F. Lecolley et al., Physics Letters B354 (1995) 202-207

[21] G. Casini et al., Phys. Rev. Lett., 71-16 (1993) 2567

[22] A.A. Stefanini et al., Zeitschrift Physik A351 (1995) 167-186

[23] P. Glassel et al., Z. Phys. A310 (1983) 189-216

[24] J. Colin et al., Nuclear Physics A593 (1995) 48-68

[25] D. Durand et al., Physics Letters B345(1995) 397-402

[26] J.C. Steckmeyer, Proceedings of the XXXVIIth Winter Meeting on Nuclear Physics, Edited by I.Iori, 25-30 January 1999, Bormio, Italy, 230-240.

[27] L.G. Moretto et al., Nuclear Physics A274 (1975) 211

[28] G. Royer et al., Nuclear Physics A466 (1987) 139-156;
G. Royer et al., Journal of physics G20 (1994) L131;
G. Royer, F. Haddad Journal of physics G21 (1995) 339-349

[29] D.J. Hinde et al., Nuclear Physics A452 (1986) 550-572
D.J. Hinde et al., Nuclear Physics A538(1992) 243c-262c

[30] D. Hilcher et al., Phys. Rev.Letters vol 62 N10 (1989) 1099-1102